Biochem. J. (1991) 277, 239–243 (Printed in Great Britain)



# Kinetics of GTP hydrolysis during the assembly of chick brain MAP2–tubulin microtubule protein

Roy G. BURNS
Biophysics Section, Blackett Laboratory, Imperial College of Science, Technology and Medicine, London SW7 2BZ, U.K.

The kinetics of GTP hydrolysis during microtubule assembly have been examined using chick brain MAP2–tubulin microtubule protein in a NaCl-supplemented buffer. The elongating microtubules terminate in a 'GTP cap', since the kinetics of GTP hydrolysis are slower than those of subunit addition. GTP hydrolysis is (*a*) stoichiometric, (*b*) occurs as a vectorial wave as the initial rate of hydrolysis is proportional to the molar concentration of microtubule ends and not to the initial rate of subunit addition, and (*c*) either does not occur, or occurs only at a much lower rate, in the terminal subunits.

## INTRODUCTION

GTP binds to an exchangeable (E-) site on β-tubulin and is hydrolysed to GDP during the assembly of pure tubulin (see, e.g., David-Pfeuty *et al.*, 1977). This hydrolysis may occur at a lower rate than the initial rate of subunit addition (see, e.g., Carlier & Pantaloni, 1981), such that the microtubule initially consists of a mixture of $Tu^{GTP}$ and $Tu^{GDP}$ (i.e. subunits with GTP or GDP bound to the E-site), whereas microtubules at steady state can consist almost exclusively of $Tu^{GDP}$. By contrast, other workers have observed that the kinetics of subunit addition and GTP hydrolysis are indistinguishable (Caplow, 1986; Murphy & Wallis, 1986; O'Brien *et al.*, 1987; Schilstra *et al.*, 1987; Stewart *et al.*, 1990).

The difference in the kinetics of GTP hydrolysis and subunit addition has led to the proposal that elongating microtubules terminate in a 'GTP cap' (Carlier & Pantaloni, 1981), and that this cap of $Tu^{GTP}$ subunits is more stable than the $Tu^{GDP}$ core (Carlier *et al.*, 1984; Chen & Hill, 1985). Stochastic loss of this cap is postulated to result in the dynamic instability observed under steady-state conditions (Mitchison & Kirschner, 1984). Indeed, a terminal GTP cap or another kinetic difference is necessary to account for the observed dynamic instability, even when there is no experimentally detectable difference between the kinetics of subunit addition and GTP hydrolysis.

The three following models have been proposed relating GTP hydrolysis to subunit addition (Carlier & Pantaloni, 1985).

(*a*) That GTP hydrolysis is fast and is tightly coupled to subunit addition such that it occurs in the terminal subunit (see, e.g., O'Brien *et al.*, 1987; Stewart *et al.*, 1990).

(*b*) That GTP hydrolysis is a random event within the subunits of the microtubule, such that there is a gradient of $Tu^{GTP}$ subunits which is maximal at the end of an elongating microtubule and minimal at the core (see, e.g., Carlier & Pantaloni, 1981).

(*c*) That GTP hydrolysis is vectorial, with a wave of hydrolysis being propagated along the elongating microtubule. This model predicts a sharp boundary between two domains, with hydrolysis in one subunit inducing it in the neighbouring subunit, and is supported by evidence that there is a maximum rate of GTP hydrolysis (Carlier *et al.*, 1987*a*, *b*). It has, however, not yet been possible to compare directly the absolute rates of subunit addition and GTP hydrolysis under conditions which indicate a substantial GTP cap.

This is addressed here. The assembly of chick brain MAP2–tubulin microtubules in a buffer supplemented with 67 mM-NaCl conform to a pseudo-first-order reaction without detectable end-to-end annealing [the preceding paper (Burns, 1991)]. This permits the association rate constant ($k_{+1}^{GTP}$) to be determined, such that the rate of subunit addition, and GTP hydrolysis can be directly compared. Hydrolysis is shown to occur vectorially, but that it does not occur, or it occurs only at a much suppressed rate, in the terminal subunit(s).

## MATERIALS AND METHODS

### Microtubule protein and kinetics of assembly

The preparation of twice-cycled chick brain microtubule protein, its composition, elution through Sephadex G-50 into an assembly buffer supplemented with 67 mM-NaCl, and the procedures used for monitoring microtubule assembly have been described previously (Islam & Burns, 1985; Burns, 1991). 'Seeds' were prepared immediately before use by shearing pre-assembled microtubules by ten passages through a 100 μl Hamilton syringe; the mean lengths were generally ≃ 1 μm. A portion was fixed with 0.1% (v/v) glutaraldehyde, negatively stained [1% (w/v) uranyl acetate], and photographed (5000–10000×; JEM 1800-EX electron microscope). All microtubules on a micrograph were measured, the length of those extending over the edge being doubled. The seed concentration was calculated from the mean length, the protein content of a pelleted aliquot, the protein composition (80% tubulin) and the molecular mass of tubulin (100 kDa), assuming that a 1 μm microtubule contains 1750 tubulin dimers.

### Kinetics of [γ-$^{32}$P]GTP hydrolysis

Microtubule assembly was initiated by adding [γ-$^{32}$P]GTP (to ≃ 100 μM) to the pre-warmed samples. The assays did not include adenosine 5′-[βγ-imido]triphosphate to inhibit various phosphatases (Caplow, 1986; Murphy & Wallis, 1986; Carlier & Pantaloni, 1982), as the purity of commercial preparations of adenosine 5′-[βγ-imido]triphosphate has been questioned (Batra *et al.*, 1987). The exact [γ-$^{32}$P]GTP concentration was determined by measuring the $A_{257}$ for a parallel assay without added microtubule protein. No correction was made for the GDP bound to the exchangeable site, as the assay did not contain a

Abbreviations and terms used: $k_{+1}^{GTP}$, $k_{-1}^{GTP}$, $C_0^{GTP}$ and $Tu^{GTP}$ are the association and dissociation rate constants, the consequential critical concentration ($k_{-1}^{GTP}/k_{+1}^{GTP}$) before GTP hydrolysis, and tubulin dimers with bound GTP; $k_{-1}^{GDP}$ is the dissociation rate constant after GTP hydrolysis; $C_0^{ss}$ is the observed critical concentration at steady state, representing the number average of the critical concentrations of microtubules with ($C_0^{GTP}$) and without a terminal 'GTP cap'; [M] is the molar concentration of microtubules; MAP, microtubule-associated protein.

GTP-regenerating system. Aliquots (50 $\mu$l) were removed, and further hydrolysis prevented by adding 10 mg of activated charcoal in 1 ml of 2.5 mM-$KH_2PO_4$/0.1 M HCl. Charcoal was used because incomplete recoveries have been reported for phosphomolybdate extraction (O'Brien *et al.*, 1987). The charcoal was pelleted (10000 *g*, 10 min), and aliquots of the supernatant removed for Čerenkov-radiation counting. The hydrolysis of [$\gamma$-$^{32}$P]GTP was expressed in terms of $\mu$M-phosphate released by comparison with the initial specific radioactivity of the [$\gamma$-$^{32}$P]GTP. The initial amount of $^{32}PO_3^{4-}$ (generally 1–3 %) was subtracted from all values.

### Protein concentrations

Protein concentrations [measured as described by Hartree (1972), with BSA as the standard] were expressed as either mg of microtubule protein $\cdot$ml$^{-1}$ or $\mu$M-tubulin dimer. The extent of microtubule assembly was expressed as $\mu$M-tubulin dimer assembled by multiplying the increase in turbidity at $A_{350}$ with the scattering coefficient (1 absorption unit = 44 $\mu$M-tubulin assembled).

### Materials

Biochemicals were purchased from Sigma Chemical Co., [$\gamma$-$^{32}$P]GTP was from Amersham International, and Sephadex G-50 was from Pharmacia Ltd.

## RESULTS

### Determination of $k_{+1}^{GTP}$

Microtubule protein (2.1 mg$\cdot$ml$^{-1}$; 16.8 $\mu$M-tubulin) was warmed to 37 °C, and assembly was initiated by the addition of 100 $\mu$M-GTP, 1 mM-phosphoenolpyruvate and pyruvate kinase (60 $\mu$g$\cdot$ml$^{-1}$; $\simeq$ 500 units$\cdot$mg$^{-1}$) and known concentrations of preformed 'seeds'. Plotting the calculated values of $k_{+1}^{GTP}$ versus the seed concentration (Fig. 1) yields an association rate constant ($k_{+1}^{GTP}$) of $40 \times 10^6$ M$^{-1}\cdot$s$^{-1}$. Similar values [$(36–41) \times 10^6$ M$^{-1}\cdot$s$^{-1}$] have been obtained in other experiments and compare very favourably with determinations based upon the direct measurement of immunostained microtubules under the same buffer conditions [the following paper (Symmons & Burns, 1991)]. No significant difference was detected when the GTP-regenerating system was omitted.

Increasing concentrations of microtubule protein were assembled to steady state with 100 $\mu$M-GTP, 1 mM-phosphoenolpyruvate and pyruvate kinase (60 $\mu$g$\cdot$ml$^{-1}$). The predicted maximum extent of assembly was determined by extrapolation of the pseudo-first-order plot (Burns, 1991) to yield $C_0^{GTP}$ (2.0 $\mu$M-tubulin; Fig. 2). At steady state, the samples were pelleted, and the protein contents determined to yield a value of $C_0^{SS}$ (3.35 $\mu$M-tubulin, Fig. 2). The assembly competency, given by the slope, was 94 %, and combining $k_{+1}^{GTP}$ and $C_0^{GTP}$ yields the dissociation rate constant $k_{-1}^{GTP}$ of 80 s$^{-1}$.

### Kinetics of GTP hydrolysis during microtubule assembly

Microtubule protein was assembled by addition of 100 $\mu$M-[$\gamma$-$^{32}$P]GTP in the absence of a GTP-regenerating system (Fig. 3). The very short lag phase ($\simeq$ 25 s) is followed by rapid assembly to steady state. Phosphate release is significantly slower than subunit addition, with an initial burst of GTPase activity which declines to a constant rate. Extrapolation of this steady-state rate to zero time shows that the extent of the initial burst is similar to the extent of microtubule assembly (12.0 $\mu$M-phosphate released; 13.0 $\mu$M-tubulin assembled).

The kinetics of the initial burst of GTP hydrolysis were analysed by subtracting the steady-state rate of phosphate release and then calculating the amount of phosphate yet to be released during the initial burst as a function of time (Fig. 4). These kinetics conform to an apparent first-order reaction, with an observed rate constant of $1.60 \times 10^{-3}$ s$^{-1}$. Different preparations of microtubule protein yielded apparent first-order rate constants of $(1.4–2.4) \times 10^{-3}$ s$^{-1}$.

This apparent first-order rate constant is consistent with either a random or a vectorial model for GTP hydrolysis. In the former case, the instantaneous rate of GTP hydrolysis would be proportional to the remaining concentration of assembled $Tu^{GTP}$. By contrast, the vectorial model predicts a constant rate of GTP hydrolysis per microtubule, but the observed rate in bulk solutions will decline with time, owing to the falling number of microtubules bearing a GTP cap. Analysis of individual microtubule lengths by indirect immunofluorescence has shown a broad population distribution (Symmons & Burns, 1991), resulting from the premature termination of elongation. The random and vectorial models can, though, be distinguished by considering the initial rate of GTP hydrolysis relative to the initial rate of subunit addition versus the initial concentration of

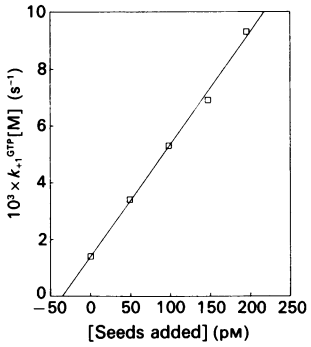


**Fig. 1. Determination of $k_{+1}^{GTP}$ by examining the pseudo-first-order rate constant ($k_{+1}^{GTP}$[M]) as a function of the concentration of exogenous seeds**

Nucleotide-depleted microtubule protein (2.1 mg$\cdot$ml$^{-1}$; 16.8 $\mu$M-tubulin) was assembled at 37 °C with 100 $\mu$M-GTP and a GTP-regenerating system, and increasing concentrations of preassembled seeds. The pseudo-first-order rate constant was calculated from the instantaneous rate of assembly as a function of the concentration of tubulin yet to be assembled (Burns, 1991).

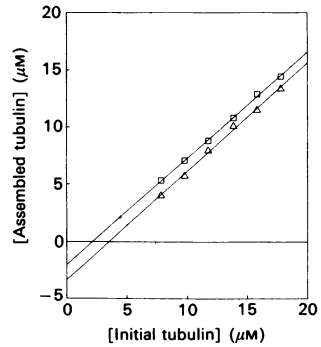


**Fig. 2. Determination of $C_0^{GTP}$ and $C_0^{SS}$**

Increasing concentrations of nucleotide-depleted microtubule protein were assembled at 37 °C with 100 $\mu$M-GTP and a GTP-regenerating system. The predicted maximum extent of assembly, to yield $C_0^{GTP}$ (□), was calculated by extrapolating the pseudo-first-order plot to the abscissa (see Burns, 1991). The microtubules were pelleted at steady state (5 min; 100000 *g*; Beckman Airfuge), and the protein concentrations measured to yield a value of $C_0^{SS}$ (△).

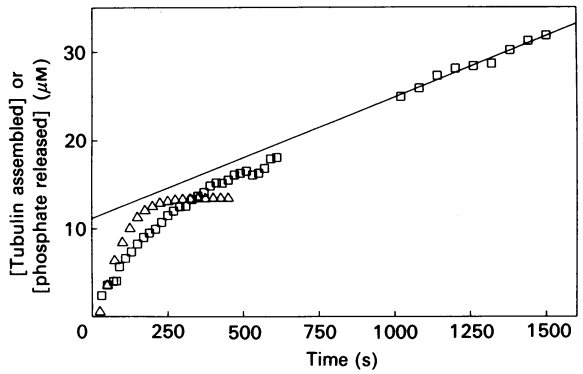


**Fig. 3. Kinetics of microtubule assembly (△) and [γ-$^{32}$P]GTP hydrolysis (□)**

Nucleotide-depleted microtubule protein (2.20 mg·ml$^{-1}$; 17.6 μM-tubulin) was assembled at 37 °C with 100 μM-[γ-$^{32}$P], monitoring the assembly by the increase in turbidity at $A_{350}$ and the kinetics of GTP hydrolysis by removing 50 μl aliquots and quenching with 1 ml of activated charcoal (10 mg·ml$^{-1}$) in 2.5 mM-$KH_2PO_4$/0.1 M-HCl. After pelleting the activated charcoal, triplicate 100 μl aliquots were counted for Čerenkov radiation, and the hydrolysis was expressed relative to the initial [γ-$^{32}$P]GTP specific radioactivity. The extent of polymerization was also expressed in μM terms by assuming that one $A_{350}$ unit equals 44 μM assembled tubulin. $^{32}PO_4^{3-}$ contamination of the [γ-$^{32}$P]GTP (1–3 %) was subtracted from all values.

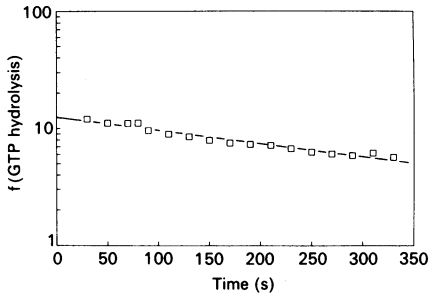


**Fig. 4. Kinetics of the initial burst of GTP hydrolysis expressed as a semi-logarithmic plot**

The extent of GTP hydrolysis (Fig. 3) during the initial burst have been corrected for the steady-state rate of GTP hydrolysis and then expressed as $\log([^{32}PO_4^{3-}]_{ss} - [^{32}PO_4^{3-}]_t)$, shown as f(GTP hydrolysis), versus time where $_{ss}$ and $_t$ refer to the values at steady state and at time $t$. The initial rate of GTP hydrolysis was calculated from the release of $^{32}PO_4^{3-}$ over the first 20 s.

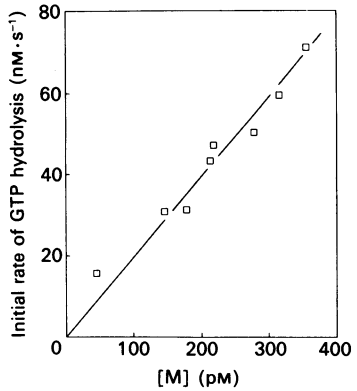


**Fig. 5. Initial rate of GTP hydrolysis as a function of the molar concentration of microtubule ends ([M]) for eight separate experiments**

The initial rate of GTP hydrolysis was calculated as described in Fig. 4, and [M] by dividing the observed pseudo-first-order rate constant ($k_{+1}^{GTP}$[M]) by $k_{+1}^{GTP}$ ($40 \times 10^6$ M$^{-1}$·s$^{-1}$). The graph has been constrained to pass through the origin.

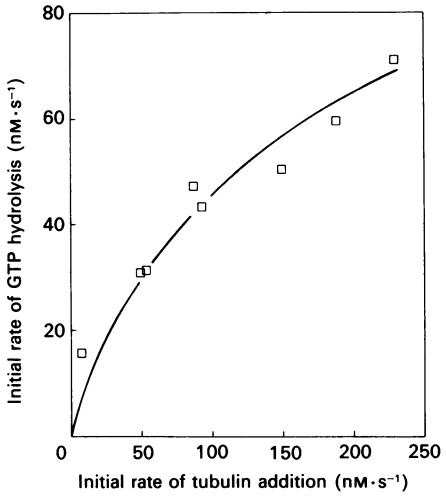


**Fig. 6. Initial rate of GTP hydrolysis as a function of the initial rate of subunit addition for eight separate experiments**

The initial rate of GTP hydrolysis was calculated as described in Fig. 4, and the initial rate of subunit addition ($k_{+1}^{GTP}$[Tu$^{GTP}$][M]) from the product of the observed pseudo-first-order constant ($k_{+1}^{GTP}$[M]) and the extent of assembly corrected for the deviation immediately before steady state (see Burns, 1991). The curve has been constrained to pass through the origin.

microtubule ends. The random model predicts that the initial rate of GTP hydrolysis would be proportional to the initial rate of subunit addition (that is, to $k_{+1}^{GTP}$[Tu$^{GTP}$][M]), whereas the vectorial model predicts that it would be proportional to [M].

The assembly kinetics permit the separation determination of [M] and $k_{+1}^{GTP}$[Tu][M]. The initial rate was calculated from the product of observed value of $k_{+1}^{GTP}$[M] and the extent of assembly at steady state, corrected for the consequences of dynamic instability (Burns, 1991). By contrast, the extent of nucleation has been calculated from the observed value of $k_{+1}^{GTP}$[M] and the determined association rate constant (Fig. 1). The initial rate of GTP hydrolysis has been derived from the intercept of the apparent first-order plot of GTP hydrolysis (see, e.g., Fig. 4). This approach utilizes the kinetics of GTP hydrolysis during the first 24 min and provides a more accurate determination of the initial rate than attempts to measure it directly.

The initial rate of GTP hydrolysis is directly proportional to the molar concentration of microtubules ([M]; Fig. 5), but not to the initial rate of subunit addition ($k_{+1}^{GTP}$[Tu$^{GTP}$][M]; Fig. 6). The former yields a value for $k_{cat.}^{GTP}$ of 200 s$^{-1}$ relative to the concentration of microtubules. Assuming that each microtubule has 13 protofilaments and a site of GTP hydrolysis at each end, $k_{cat.}^{GTP}$ equals 7.7 s$^{-1}$ relative to the tubulin dimer.

The extent of the GTP burst has been examined as a function of the steady-state extent of microtubule assembly (Fig. 7). Although there is some experimental variation, the mean stoichiometry is 0.97 mol of GTP hydrolysed per mol of tubulin dimer added. The intercept (1.0 μM-tubulin) is probably due to the small increase in turbidity which is observed even in the absence of GTP and which is not due to microtubule assembly. Indeed, close examination of the data suggests that much of the observed scatter is due to variation in the extent of this assembly-incompetency.

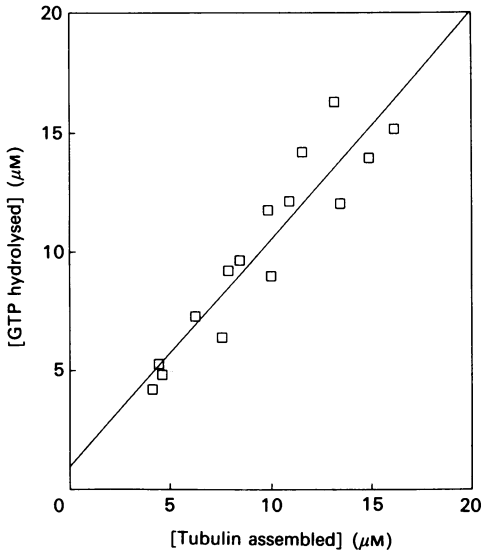


**Fig. 7. Stoichiometry of the initial burst of GTP hydrolysis**

The magnitude of the GTP burst was determined by extrapolating the steady-state rate to 0 s (Fig. 3), and the extent of assembly from the pseudo-first-order plot without correcting for the deviation immediately before steady state. The slope represents the hydrolysis of 0.97 mol of [$\gamma$-$^{32}$P]/mol of assembled tubulin dimer.

## DISCUSSION

The rate of phosphate release observed at steady state may include hydrolysis due to contaminating activities as well as that resulting from continued subunit addition. The analysis therefore assumes that neither activity is affected by the depletion of GTP or the generation of GDP; no apparent inhibition is observed (15–24 min; Fig. 3). Such concomitant hydrolysis, provided that it is at a constant rate, does not affect estimates of the magnitude of the initial burst or the initial rate.

The magnitude of the initial GTP burst (0.97 mol·mol$^{-1}$; Fig. 7) is similar to that reported for the assembly of pure tubulin (O'Brien *et al.*, 1987; Schilstra *et al.*, 1987; Carlier *et al.*, 1987) or during the assembly of a preformed tubulin–GTP complex (MacNeal & Purich, 1978). This stoichiometry provides an internal control of the efficiency of phosphate capture by the activated charcoal and for the absorption coefficient used to calculate the concentration of assembled microtubules.

The difference between the kinetics of subunit addition and GTP hydrolysis is similar to that reported for the assembly of pure tubulin (Carlier *et al.*, 1987) and confirms that elongating MAP2–tubulin microtubules terminate in a GTP cap. By contrast, workers in other laboratories have noted little difference between the kinetics of subunit addition and GTP hydrolysis (Caplow, 1986; Murphy & Wallis, 1986; O'Brien *et al.*, 1987; Schilstra *et al.*, 1987; Stewart *et al.*, 1990). The specific criticisms levelled against earlier evidence for a GTP cap (O'Brien *et al.*, 1987) do not apply to the current work, as the hydrolysis is stoichiometric (Fig. 7), the lag phase is short and the kinetics have been plotted on the same axes (Fig. 3).

The failure by various workers to detect a significant GTP cap may simply be a direct consequence of the precise buffer conditions and protein composition. For instance, in two studies in which the authors were unable to detect a terminal GTP cap on pure tubulin microtubules (Murphy & Wallis, 1986; Stewart *et al.*, 1990) the net association rate constants were only $11 \times 10^6$ M$^{-1}$·s$^{-1}$ (Rothwell *et al.*, 1986) and $9.8 \times 10^6$ M$^{-1}$·s$^{-1}$ (Stewart *et al.*, 1990). Although the latter workers used high protein concentrations (45–79 $\mu$M-tubulin), the achieved rates (< 800 s$^{-1}$) were less than those in the current study. Other studies also indicate that the buffer and/or protein composition may be relevant factors. For example, a difference between the kinetics of subunit addition and GTP hydrolysis could be detected using pure brain tubulin at pH 7.0, but not at pH 6.0 (Hamel *et al.*, 1986). By contrast, porcine brain tubulin assembled in 3.4 M-glycerol, with an association rate constant of only $\simeq 5 \times 10^6$ M$^{-1}$·s$^{-1}$, exhibited a GTP cap at protein concentrations exceeding 7 $\mu$M-tubulin (Carlier *et al.*, 1987), that is, when the maximum rate of subunit addition was only $\simeq$35 dimers·s$^{-1}$. A GTP cap would be indetectable under the current conditions at such a low elongation rate, indicating that either GTP hydrolysis occurs more slowly in the glycerol buffer or that the rate of subunit addition was underestimated.

Analysis of the initial rates of subunit addition and GTP hydrolysis has established that GTP hydrolysis is a vectorial process (Figs. 5 and 6). This differs from an apparently similar conclusion (Caplow, 1986) in that the earlier study concluded that the hydrolysis occurred in the terminal subunit(s), but is in agreement with the demonstration that the maximum rate of GTP hydrolysis can be lower than that of subunit addition (Carlier *et al.*, 1987). The kinetics of phosphate release yield a value of 200 s$^{-1}$ (Fig. 5), which equals a $k_{cat.}^{GTP}$ of 7.7 s$^{-1}$ relative to the tubulin dimer. This rate is equivalent to the vectorial wave migrating along the microtubule at 62 nm·s$^{-1}$. The observed $k_{cat.}^{GTP}$ is significantly lower than a minimum rate (38 s$^{-1}$) computed to account for the absence of a detectable GTP cap on pure tubulin microtubules (Stewart *et al.*, 1990). This suggests that either the current buffer conditions or the presence of MAP2 suppresses the rate of GTP hydrolysis. As transmission of the vectorial wave of GTP hydrolysis is presumably effected by a induced conformational change, it is highly probable, although unproven, that this may be inhibited by the interaction with MAP2.

A declining rate of GTP hydrolysis is observed (Figs. 2). As GTP hydrolysis is a vectorial process, this declining rate reflects the decrease in the number of microtubules with a terminal GTP cap. The exponential decay therefore indicates that a significant number of microtubules join the subpopulation lacking a terminal GTP cap from the earliest stages of the elongation phase. This is confirmed by the broad spread of individual microtubule lengths of samples prepared for immunostaining before the onset of steady state (Symmons & Burns, 1991). The half-life of this decay (400–700 s) is somewhat higher than a computed value (240 s; Carlier & Pantaloni, 1981) and very much higher than a prediction (< 20 s) based on the behaviour of microtubules lacking a detectable GTP cap (O'Brien *et al.*, 1987), both of which took into account that the hydrolysis is the second of two sequential reactions.

The rate of GTP hydrolysis at steady state reflects the sum of (*a*) the hydrolysis by assembly-independent activities, and (*b*) assembly-dependent hydrolysis due to the continued addition of tubulin subunits, at a rate proportional to the molar concentration of microtubule ends. Different preparations of microtubule protein yielded steady-state rates of GTP hydrolysis/microtubule of 46 s$^{-1}$ ($n$ = 10) and 52.5 s$^{-1}$ ($n$ = 6), that is, rates which are substantially lower than that during the rapid elongation phase.

The fraction of microtubules continuing to elongate at steady state ($n$) can be calculated from:

$$k_{-1}^{GTP}(1-n) = n(k_{+1}^{GTP}[Tu^{GTP}] - k_{-1}^{GTP})$$

Incorporating the derived numerical values [$k_{+1}^{GTP} = 40 \times 10^6$ M$^{-1}$·s$^{-1}$ (Fig. 1), $k_{-1}^{GTP} = 80$ s$^{-1}$ (Fig. 2), the free tubulin concentration ($C_0^{SS}$) = 3.35 $\mu$M (Fig. 2), and $k_{-1}^{GDP} = 350$ s$^{-1}$;

Symmons & Burns, 1991] shows that $\simeq 87\%$ of the microtubules are elongating at the expense of $\simeq 13\%$ which are dissociating; that is, $\simeq 49$ subunits are gained or lost per second per microtubule. Consequently, the predicted steady-state rate of GTP hydrolysis is very similar to the observed rate (46–52.5 $s^{-1}$). This strongly suggests that there is minimal GTPase contamination and that the rate of GTP hydrolysis is limited, under steady-state conditions, by the rate of subunit addition, as predicted by the lateral cap model (Bayley *et al.*, 1990). One consequence is that the kinetics of GTP hydrolysis, with respect to a single microtubule, must be biphasic, occurring at 200 $s^{-1}$ during elongation but slowing to $\simeq 50$ $s^{-1}$ at steady state. Such biphasic kinetics have recently been predicted (Caplow & Shanks, 1990) on the basis of modelling previously obtained data.

These biphasic kinetics are also indicated by the behaviour of the MAP2–tubulin microtubules assembled to steady state and then sheared. The microtubules exhibit length redistribution without net polymerization (Burns, 1991), owing to dynamic instability rather than end-to-end annealing. This length redistribution would be inconsistent with the calculated and observed rates of subunit addition if GTP hydrolysis in the terminal subunit occurred at the measured rate (200 $s^{-1}$) and resulted in the transition between the elongating and shortening subpopulations (catastrophe; Walker *et al.*, 1988). Consequently, GTP hydrolysis in the terminal subunit(s) must occur more slowly than that determined from the elongation kinetics. Indeed, without such a mechanism limiting GTP hydrolysis as steady state is approached, the initial burst of GTP hydrolysis would be superstoichiometric rather than the observed 0.97 $mol \cdot mol^{-1}$, owing to the re-addition of subunits dissociating from the elongating microtubules.

Direct observation of pure tubulin microtubules shows that catastrophe is an infrequent process (Horio & Hotani, 1986; Walker *et al.*, 1988). Models predicting this transition frequency and for the observed oscillations in the extent of assembly should therefore recognize that (*a*) GTP hydrolysis is a vectorial process migrating along the microtubule at constant rate, and (*b*) GTP hydrolysis in the terminal subunit(s) occurs much more slowly. Only the second of these phases would be detected under conditions, such as the assembly of pure tubulin, which only permit comparatively slow subunit addition per microtubule and a high value of $k_{cat.}$. This would lead to the erroneous conclusion that GTP hydrolysis is always induced by the addition of a subunit to the microtubule end.

Received 19 September 1990/11 January 1991; accepted 22 January 1991

## REFERENCES


Batra, J. K., Lin, C.-M. & Hamel, E. (1987) Biochemistry **26**, 5925–5931

Bayley, P. M., Schilstra, M. J. & Martin, S. R. (1990) J. Cell Sci. **95**, 33–48

Burns, R. G. (1991) Biochem. J. **277**, 231–238

Caplow, M. (1986) Ann. N.Y. Acad. Sci. **466**, 510–518

Caplow, M. & Shanks, J. (1990) J. Biol. Chem. **265**, 8935–8941

Carlier, M.-F. & Pantaloni, D. (1981) Biochemistry **20**, 1918–1924

Carlier, M.-F. & Pantaloni, D. (1982) Biochemistry **21**, 1215–1224

Carlier, M.-F. & Pantaloni, D. (1985) in Microtubules and Microtubule Inhibitors (de Brabender, M. & de May, J., eds.), pp. 61–70, Elsevier Science Publishers, Amsterdam

Carlier, M.-F., Hill, T. L. & Pantaloni, D. (1984) Proc. Natl. Acad. Sci. U.S.A. **81**, 771–775

Carlier, M.-F., Melki, R., Pantaloni, D., Hill, T. L. & Chen, Y. (1987*a*) Proc. Natl. Acad. Sci. U.S.A. **84**, 5257–5261

Carlier, M.-F., Didry, D. & Pantaloni, D. (1987*b*) Biochemistry **26**, 4428–4437

Chen, Y.-D. & Hill, T. L. (1985) Proc. Natl. Acad. Sci. U.S.A. **82**, 4127–4131

David-Pfeuty, T., Erickson, H. P. & Pantaloni, D. (1977) Proc. Natl. Acad. Sci. U.S.A. **74**, 5372–5376

Hamel, E., Batra, J. K., Huang, A. B. & Lin, C. M. (1986) Arch. Biochem. Biophys. **245**, 316–330

Hartree, E. F. (1972) Anal. Biochem. **48**, 422–426

Horio, T. & Hotani, H. (1986) Nature (London) **321**, 605–607

Islam, K. & Burns, R. G. (1985) Biochem. J. **232**, 651–656

MacNeal, R. K. & Purich, D. L. (1978) J. Biol. Chem. **253**, 4683–4687

Mitchison, T. & Kirschner, M. W. (1984) Nature (London) **312**, 237–242

Murphy, D. B. & Wallis, K. T. (1986) J. Cell Biol. **103**, 132a

O'Brien, E. T., Voter, W. A. & Erickson, H. P. (1987) Biochemistry **26**, 4148–4156

Schilstra, M. J., Martin, S. R. & Bayley, P. M. (1987) Biochem. Biophys. Res. Commun. **147**, 588–595

Stewart, R. J., Farrell, K. W. & Wilson, L. (1990) Biochemistry **29**, 6489–6498

Symmons, M. F. & Burns, R. G. (1991) Biochem. J. **277**, 245–253

Walker, R. A., O'Brien, E. T., Pryer, N. K., Soboeiro, M. F., Voter, W. A., Erickson, H. P. & Salmon, E. D. (1988) J. Cell Biol. **107**, 1437–1448